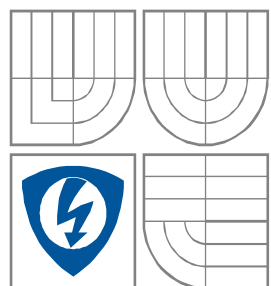


VYSOKÉ UČENÍ TECHNICKÉ V BRNĚ
BRNO UNIVERSITY OF TECHNOLOGY



FAKULTA ELEKTROTECHNIKY A KOMUNIKAČNÍCH
TECHNologiÍ

ÚSTAV RADIOELEKTRONIKY

FACULTY OF ELECTRICAL ENGINEERING AND
COMMUNICATION

DEPARTMENT OF RADIO ELECTRONICS

ŠIROKOPÁSMOVÁ PLANÁRNÍ ANTÉNA Z METAMATERIÁLŮ

BROADBAND PLANAR ANTENNA BASED ON METAMATERIAL

BAKALÁŘSKÁ PRÁCE

BACHELOR'S THESIS

AUTOR PRÁCE
AUTHOR

ISIDORO DOMINGOS

VEDOUCÍ PRÁCE
SUPERVISOR

prof. Dr. Ing. ZBYNĚK RAIDA

BRNO, 2010

ABSTRACT

The thesis deals with basic principles of meta-materials, which exhibit unusual properties in microwave applications (e.g., negative permittivity and permeability). Different types of meta-material antennas and parameters of such antennas are described in the thesis.

ABSTRAKT

V této práci se zabývám základními principy meta-materiálů. Meta-materiály vykazují neobvyklé vlastnosti v mikrovlnných aplikacích (např. negativní permitivitu a permeabilitu). V práci jsou popsány různé typy meta-materiálových antén a parametry těchto antén.

KEYWORDS

Meta-material antennas, planar antennas, negative permittivity, negative permeability.

KLÍČOVÁ SLOVA

Meta-materiálové antény, planární antény, záporná permitivita, záporná permeabilita.

DOMINGOS, I. Širokopásmová planární anténa z meta-materiálů. Semestrální projekt. Vysoké učení technické v Brně, Fakulta elektrotechniky a komunikačních technologií, Ústav radioelektroniky, 2011. Vedoucí práce: prof. Dr. Ing. Zbyněk Raida.

CONTENTS

1 INTRODUCTION	- 5 -
2 FUNDAMENTAL THEORIES OF METAMATERIALS.....	- 6 -
3 DESIGN CONSIDERATIONS	- 13 -
4 ANTENNA DESIGN	- 14 -
5 SIMULATION AND MEASUREMENT RESULTS	- 16 -
5 CONCLUSIONS.....	- 22 -
REFERENCES	- 23 -
LIST OF FIGURES	- 24 -
LIST OF SYMBOLS:	- 25 -

1 INTRODUCTION

The first attempt to explore the concept of “artificial” materials appears to trace back of the nineteenth century when in 1898 Jagadis Chunder Bose conducted the first microwave experiment on twisted structures – geometries that were essentially artificial elements by today’s terminology [1].

Meta-material (MTM) is very attractive for the design of compact antennas and microwave devices. In order to satisfy the various demands for wireless services, compact antennas with wide bandwidth and good radiation characteristics are needed.

In this project, I designed different equivalent circuits for composite right/left-handed transmission lines (CRLH-TL) that provides a conceptual route for implementing small zeroth-order resonator (ZOR) antenna.

2 FUNDAMENTAL THEORIES OF METAMATERIALS

In 1914, Lindman worked on “artificial” chiral elements media by embedding many randomly oriented small wire helices in a host medium [2]. In 1948, Kock [3] lightweight microwave lenses by arranging conducting spheres, disks, and strips periodically and effectively tailoring the effective refractive index of the artificial media. Since then, artificial complex materials have been the subject of research of many investigators worldwide. In recent years new concepts in synthesis and novel fabrication techniques have allowed the construction of structures and composite materials that mimic known material responses or that qualitatively have new, physically realizable response functions that do not occur or may not be readily available in nature.

In particulate composite media, electromagnetic waves interact with the inclusions, inducing electric and magnetic moments, which in turn affect the microscopic effective permittivity and permeability of the bulk composite “medium”. Since metamaterials can be synthesized by embedding artificially fabricated inclusions in a specified host medium or on host surface, this provides the designer with a large collection of independent parameters (or degrees of freedom)-such as the properties of the host materials; the size, shape, and composition of the inclusions; and the density, arrangement and alignment of these inclusions- to work with in order to engineer a metamaterial with specific electromagnetic response functions not found in each of the individual constituents.

In 1967, Veselago theoretically investigated plane-wave propagation in a material whose permittivity and permeability were assumed to be simultaneously negative [4]. His theoretical study showed that for monochromatic uniform plane wave in such a medium the direction of the Poynting vector is antiparallel to the direction of the phase velocity, contrary to the case of plane-wave propagation in conventional simple media.

Metamaterials with negative permittivity and permeability, several names and terminologies have been suggested, such as “left-handed” media [4-10]; media with negative refractive index [4-7, 9]; “backward-wave media” (BW media) [11]; and “double-negative (DNG)” metamaterials [12], to name a few.

To describe these properties by defining the macroscopic parameters permittivity ϵ and permeability μ of these materials. This allows for the classification of a medium as follows. A medium with both permittivity and permeability greater than zero ($\epsilon > 0$, $\mu > 0$) will be designated a double-positive (DPS) medium. Most naturally occurring media (e.g., dielectrics) fall under this designation.

This medium classification can be illustrated in the Fig. 1

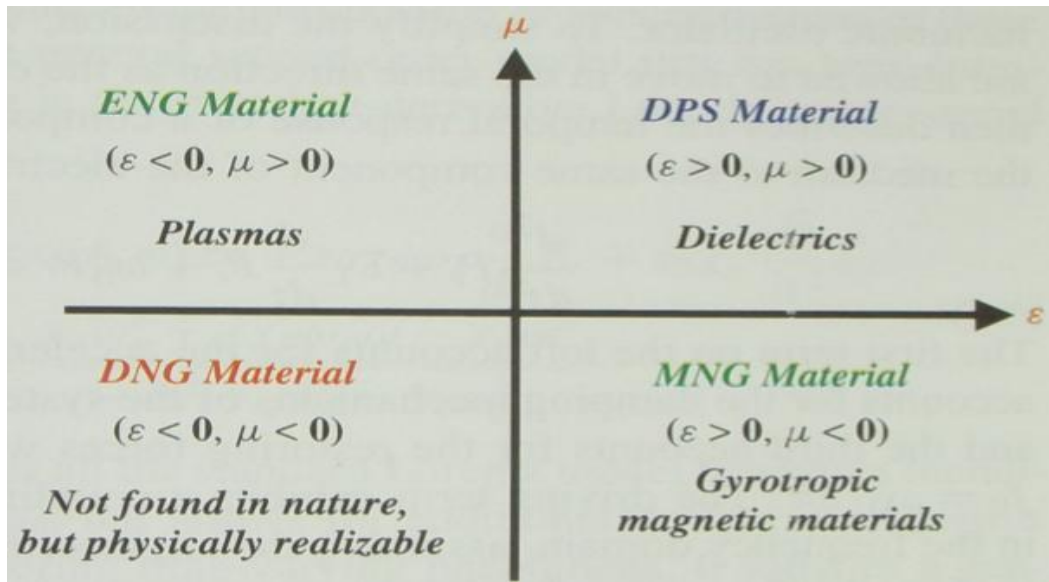


Fig. 1 Material classifications

A medium with permittivity less than zero and permeability greater than zero ($\epsilon < 0$, $\mu > 0$) will be designated an epsilon-negative (ENG) medium. In certain frequency regimes many plasmas exhibit this characteristic. Examples for noble metals (e.g., silver, gold) behave in this manner in the infrared (IR) and visible frequency domains. A medium with the permittivity greater than zero and permeability less than zero ($\epsilon > 0$, $\mu < 0$) will be designated a mu-negative (MNG) medium. Certain frequency regimes some gyrotropic materials exhibit this characteristic. Artificial materials have been constructed that also have PDS, ENG and MNG properties. A medium with the permittivity and permeability less than zero ($\epsilon < 0$, $\mu < 0$) will be designated a DNG medium.

2.1 Directivity

In the 1983 version of the IEEE Standard Definitions of Terms for Antennas, there has been a substantive change in the definition of directivity, compared to the definition of the 1973 version. Basically the term directivity in the new 1983 version has been used to replace the term directive gain of the old 1973 version. In the new 1983 version the term directive gain has been deprecated. According to the authors of the new 1983 standards, “this change brings this standard in line with common usage among antenna engineers and with other international standards, notably those of the International Electrotechnical Commission (IEC) “. Therefore directivity of an antenna defined as “the ratio of the radiation intensity in a given direction from the antenna to the radiation intensity averaged over all directions. The average radiation intensity is equal to the total power radiated by the antenna divided by 4π . If the direction is not specified, the direction of maximum radiation intensity is implied. “ Stated more simply, the directivity of a nonisotropic source is equal to the ratio of its radiation intensity in a given direction over that of isotropic source. In mathematical form, using (2-15), it can be written as

$$D = \frac{U}{U_0} = \frac{4\pi U}{P_{rad}} \quad (2-1)$$

If the direction is not specified, it implies the direction of maximum radiation intensity (maximum directivity) expressed as

$$D_{\max} = D_0 = \frac{U_{\max}}{U_0} = \frac{U_{\max}}{U_0} = \frac{4\pi U_{\max}}{P_{rad}} \quad (2-2)$$

D = directivity (dimensionless)

D₀ = maximum directivity (dimensionless)

U = radiation intensity (W/unit solid angle)

U_{max} = maximum radiation intensity (W/unit solid angle)

U₀ = radiation intensity of isotropic source (W/unit solid angle)

P_{rad} = total radiated power (W)

For antennas with orthogonal polarization components, we define partial directivity of an antenna for a given polarization in a given direction as “that part of the radiation intensity corresponding to a given polarization divided by the total radiation intensity averaged over all directions.” With this definition for the partial directivity, then in a given direction “the total directivity is the sum of the partial directivities for any two orthogonal polarizations.” For a spherical coordinate system, the total maximum directivity D_0 for the orthogonal θ and ϕ components of an antenna can be written as

$$D_0 = D_\theta + D_\phi \quad (2-3)$$

while the partial directivities D_θ and D_ϕ are expressed as

$$D_\theta = \frac{4\pi U_\theta}{(P_{rad})_\theta + (P_{rad})_\phi} \quad (2-4)$$

$$D_\phi = \frac{4\pi U_\phi}{(P_{rad})_\theta + (P_{rad})_\phi} \quad (2-5)$$

where

U_θ = radiation intensity in a given direction contained in θ field component

D_ϕ = radiation intensity in a given direction contained in ϕ field component

$(P_{rad})_\theta$ = radiated power in all directions contained in θ field component

$(P_{rad})_\phi$ = radiated power in all directions contained in ϕ field component.

2.2 RADIATION EFFICIENCY, Q, BANDWIDTH AND SIGNAL-TO NOISE RATIO

We noted that the gain G of an antenna with respect to an isotropic source is identical with antenna's directivity D provided by no losses other than radiations are present. For the more general case we write as that:

$$G = kD \quad (2-6)$$

Where k is efficiency factor ($0 \leq k \leq 1$), dimensionless

For lossless antenna, $k = 1$, but with ohmic losses k is less than 1.

If an antenna has a radiation resistance R_r and a loss R_L , then its (radiation)

$$k = \frac{R_r}{R_r + R_L} \quad (2-7)$$

and the gain

$$G = \frac{R_r}{R_r + R_L} \times \frac{4\pi A_{em}}{\lambda^2} = \frac{4\pi A_{em} k}{\lambda^2} \quad (2-8)$$

For antennas which are small compared to the wavelength, the radiation resistance R_r is small and, if ohmic losses R_L are significant, radiation efficiency is reduced. Thus, short dipoles and small loops may be inefficient radiators when losses are present. For example, when $R_r = R_L$ the radiation efficiency is 50 percent; only half of the power input to the antenna is radiated, the other half being dissipated as heat in the antenna structure.

An rf wave entering a conductor attenuates to $1/e$ of its surface value in a distance δ given by (Kraus-1),

$$\delta = \frac{1}{\sqrt{f\pi\mu\sigma}} = \text{depth of penetration} \quad (2-9)$$

where

f = frequency, Hz

μ = permeability of medium, Hm^{-1}

σ = conductivity of medium, Sm^{-1}

It is assumed that $\sigma \gg \omega \epsilon$. The induced current density in the conductor also attenuates in the same way. This means that the current density associated with a wave traveling along a conductor is greatest closed to the surface, the so-called skin effect. The quantity δ is referred to as the 1/e depth of penetration. It follows that the rf resistance of a round wire or solid cylindrical conductor equivalent to the dc resistance of a hollow tube of the same material of wall thickness δ . It is assumed that the wire or conductor diameter is much larger than δ . Assuming that the perimeter or circumference L is much smaller than the wavelength so that the current is essentially uniform around the loop, the ohmic (or loss resistance) of a small loop antenna is given by

$$R_L = \frac{L}{\sigma \pi d \delta} = \frac{L}{d} \sqrt{\frac{f \mu_0}{\pi \sigma}} \quad (2-10) \quad (\Omega)$$

where

L = loop length (perimeter or circumference), m

d = wire or conductor diameter, m

The radiation resistance of a small loop is

$$R_r \cong 31,200 \left(\frac{A}{\lambda^2} \right)^2 \cong 197 C_\lambda^4 \quad (2-11)$$

where

A = loop area (square or circular), m²

$C_\lambda = C/\lambda$, where C is circumference of circular loop.

The loop's inductive reactance is balanced by a capacitor, the terminal impedance will be resistive and equal to

$$R_T = R_r + R_L \quad (2-12)$$

And the radiation efficiency, or ratio of power radiated to input power, will be

$$k = \frac{1}{1 + \left(\frac{R_L}{R_r} \right)}$$

For a 1-turn copper-conductor circular loop (perimeter L=C) in air ($\sigma = 5.7 \cdot 10^7 \text{ } \Omega\text{m}^{-1}$, $\mu = 4\pi \cdot 10^{-7} \text{ Hm}^{-1}$),

$$\frac{R_L}{R_r} = \frac{3430}{C^3 f_{\text{MHz}}^{3.5} d} \quad (2-13)$$

where

C = circumference of loop, m

f_{MHz} = frequency, MHz d = wire (or conductor) diameter, m

For small square loops of side length l (L = 4l), we may take C = 3.5l

2.3 NEGATIVE REFRACTION

The phenomenon of negative refraction is studied by considering the scattering of a wave that is obliquely incident on a DPS-DNG interface as shown in Fig. 2. Enforcing the electromagnetic boundary condition at the interface, one obtains the law of reflection and Snell's Law from phase matching:

$$\theta_{refl} = \theta_{inc} \quad \theta_{trans} = \text{sgn}(n_2) \sin^{-1} \left(\frac{n_1}{|n_2|} \sin \theta_{inc} \right) \quad (2-14)$$

Note that if the index of refraction of a medium is negative, then the refracted angle, according to Snell's Law, should also become "negative". This suggests that the refraction is anomalous, and the refracted angle is on the same side of the interface normal as the incident angle is. The wave and the Poynting vectors associated with this oblique scattering problem are also obtained:

$$k_{inc} = k_1 (\cos \theta_{inc} z + \sin \theta_{inc} x)$$

$$k_{refl} = k_1 (-\cos \theta_{inc} z + \sin \theta_{inc} x)$$

$$k_{trans} = k_2 (\cos \theta_{trans} z + \sin \theta_{trans} x)$$

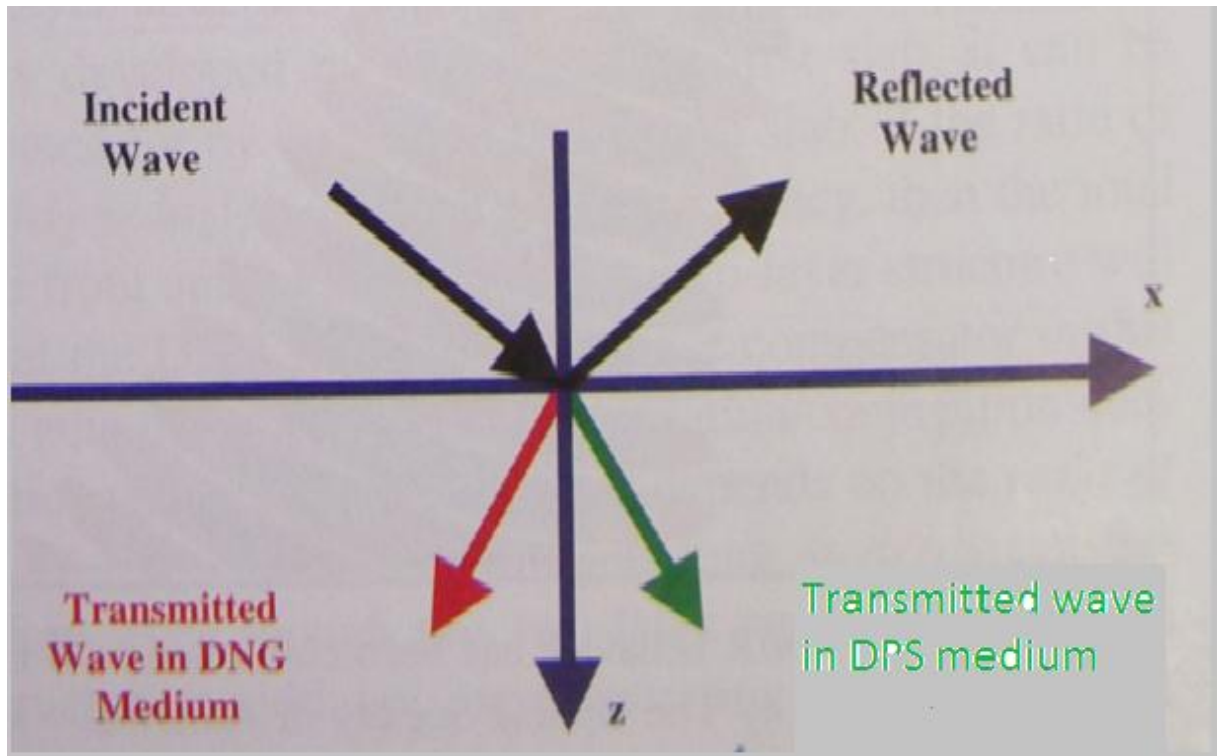


Fig. 2 Geometry of the scattering of a wave obliquely incident upon a DPS-DNG interface

3 DESIGN CONSIDERATIONS

The design of MTM antennas is based on the CRLH-TL unit cell shown in Fig. 1. It consists of a conventional host TL with characteristic impedance Z_0 and physical length d loaded with series capacitance C_L and shunt inductance L_L . The conventional host TL has intrinsic series inductance L_R and shunt capacitance C_R .

The analytical dispersion equation of the CRLH-TL can be obtained by applying the Bloch and Floquet theory to the unit cells as follows [1]:

$$\cos(\beta d) = 1 - \frac{1}{2} \frac{(\omega^2 - \omega_{se}^2)(\omega^2 - \omega_{sh}^2)}{\omega^2 \omega_R^2}. \quad (3-1)$$

Here, $\omega_{se} = 1/\sqrt{L_R C_L}$, $\omega_{sh} = 1/\sqrt{L_L C_R}$, and $\omega_R = 1/\sqrt{L_R C_R}$. Further, β is the propagation constant for Bloch waves, and d is the length of the unit cell. The resonance of the CRLH-TL for resonance modes n can be obtained by the following condition [1]:

$$\beta_n d = \frac{n\pi d}{l} = \frac{n\pi}{N}, \quad n = 0 \pm 1, \pm 2, \dots, (N-1). \quad (3-2)$$

Here, N and l are the number of unit cells and the total length of the resonator, respectively.

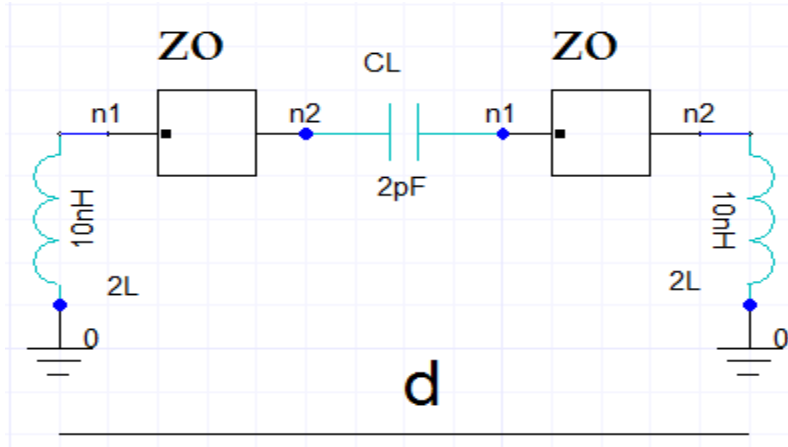


Fig.3 Equivalent circuit model for the ideal CRLH-TL unit cell.

4 ANTENNA DESIGN

In this project, I designed one configuration of meta-material antenna. The investigated configuration is shown in Fig. 2. The antennas differ in the value of the serial inductance, which is given by the number of meanders, and in the value of the serial capacitance, which is given by the length of the gap g between cells. The described configurations were numerically analyzed in Ansoft Designer.

The antennas are based on two simplified planar mushroom structure unit cells. The unit cell is composed of a host TL with a gap and a metal strip line with a meander inductor. The gap on the host TL acts like C_L , and the metal strip lines with meander inductors behave like L_L . The host TLs can possess the right-handed parasitic effect that can be seen as L_R and C_R . For the fixed host TLs and metal strip lines, the zeroth-order resonance frequency is determined by lumped inductors.

The antenna was constructed with the following parameters:
ARLON 25N, $\epsilon_r = 3,38$ and $h = 1,54\text{mm}$.

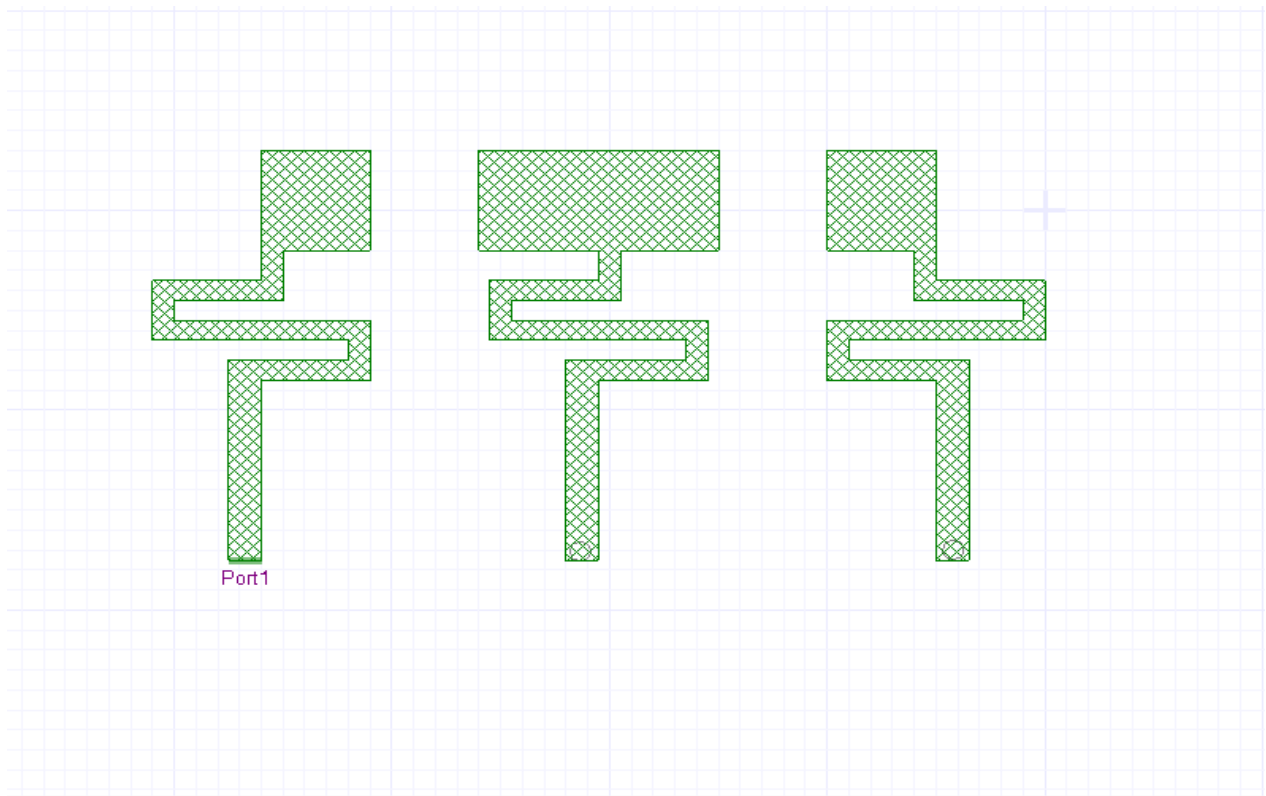


Fig. 4 MTM antenna with extended bandwidth.

Fig. 5 shows the simulated return loss for the transmission line with the gap width $g = 3$ mm.

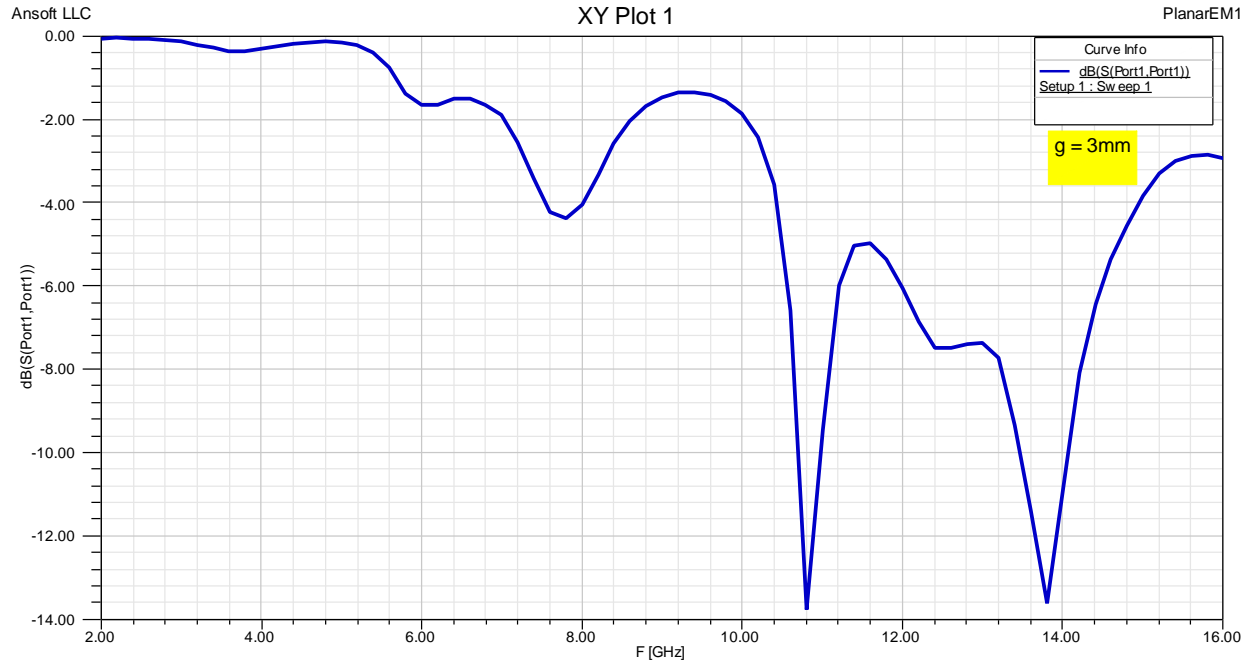


Fig. 5 Simulated return loss for the transmission line with the gap width $g = 3$ mm. Analysis performed from 2 GHz to 16 GHz and frequency step 0.2 GHz.

5 SIMULATION AND MEASUREMENT RESULTS

The simulation results (frequency response of return loss) are the same for all gaps varying from 1 mm to 5 mm when investigations are performed in the frequency range from 2 GHz to frequency 16 GHz and the frequency step 0.2 GHz.

For the antenna (Fig. 4), the operating frequency is 13.8 GHz. While the zeroth-order resonance frequency is not changed, the first-negative-order resonance frequency is increased from 7.8 GHz, 11 GHz to 13.8 GHz for $g = 1$ mm, 3 mm and $g = 5$ mm, respectively.

In order to verify the resonance modes of the antenna, current distributions and directivity patterns were investigated at the frequencies 13.8 GHz and 7.8 GHz (see Fig. 6, Fig 6a and Fig 6b).

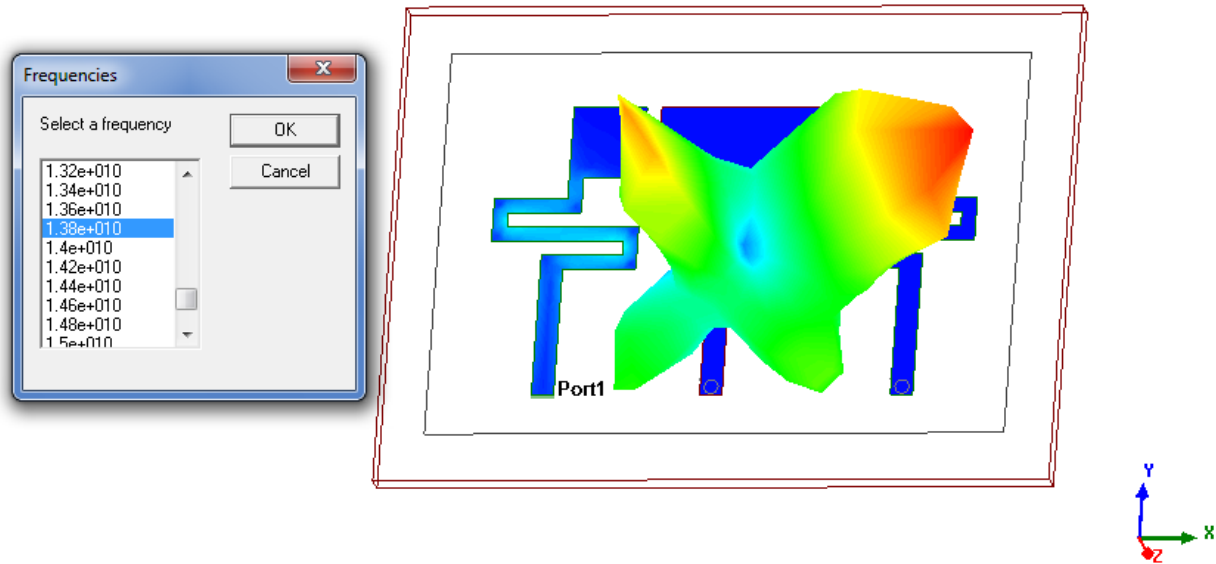


Fig. 6 The simulated surface current distribution and directivity pattern of the antenna with $f = 13.8$ GHz.

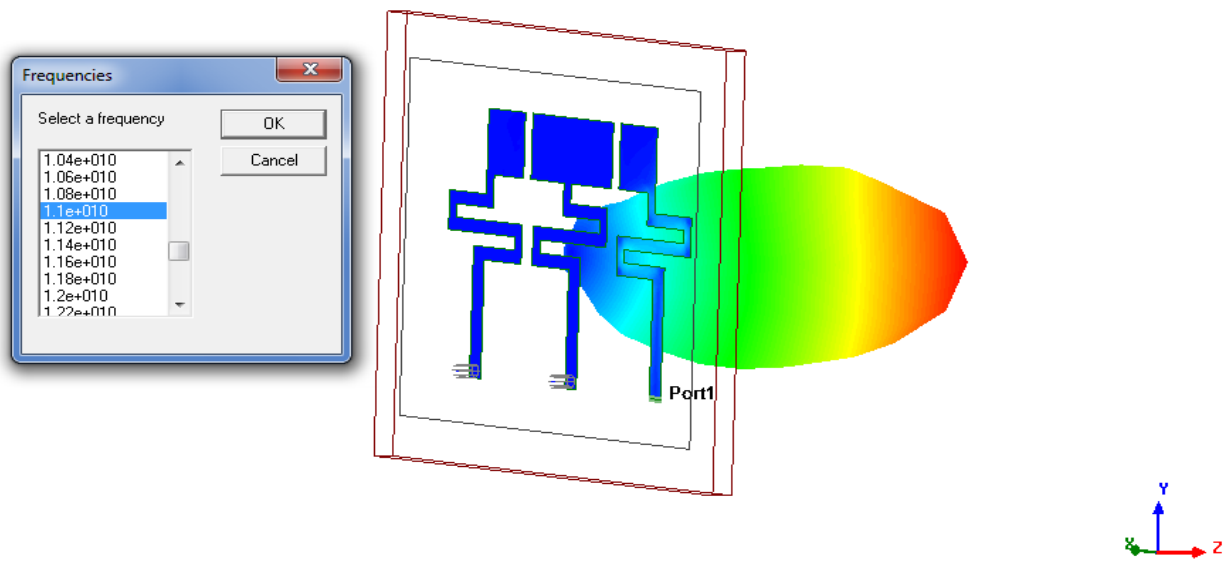


Fig. 6a The simulated surface current distribution and directivity pattern of the antenna with $f = 11$ GHz.

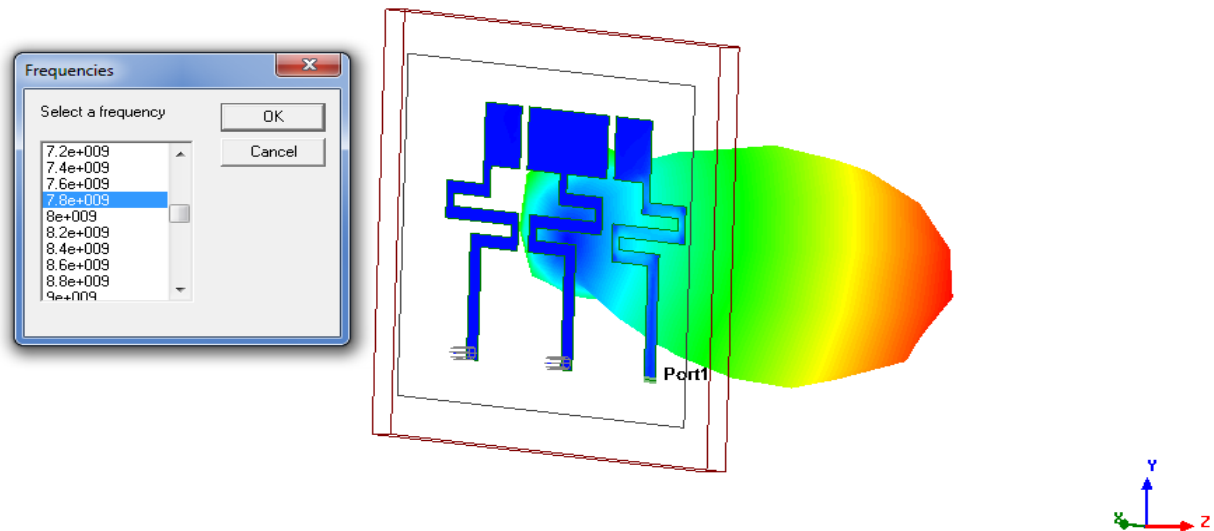
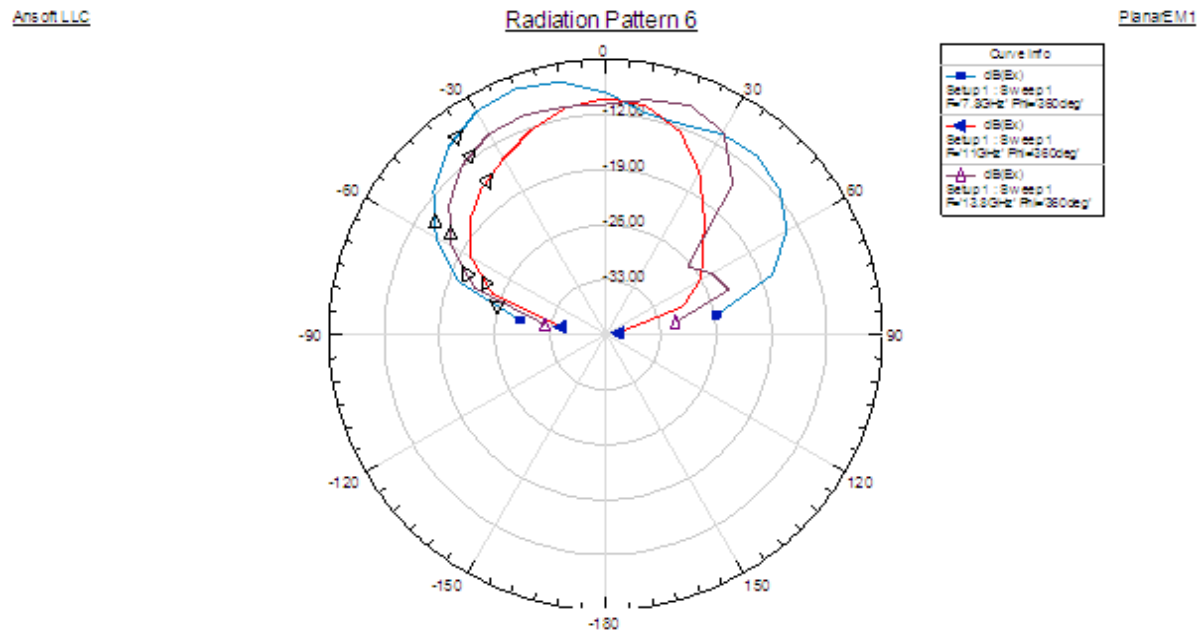
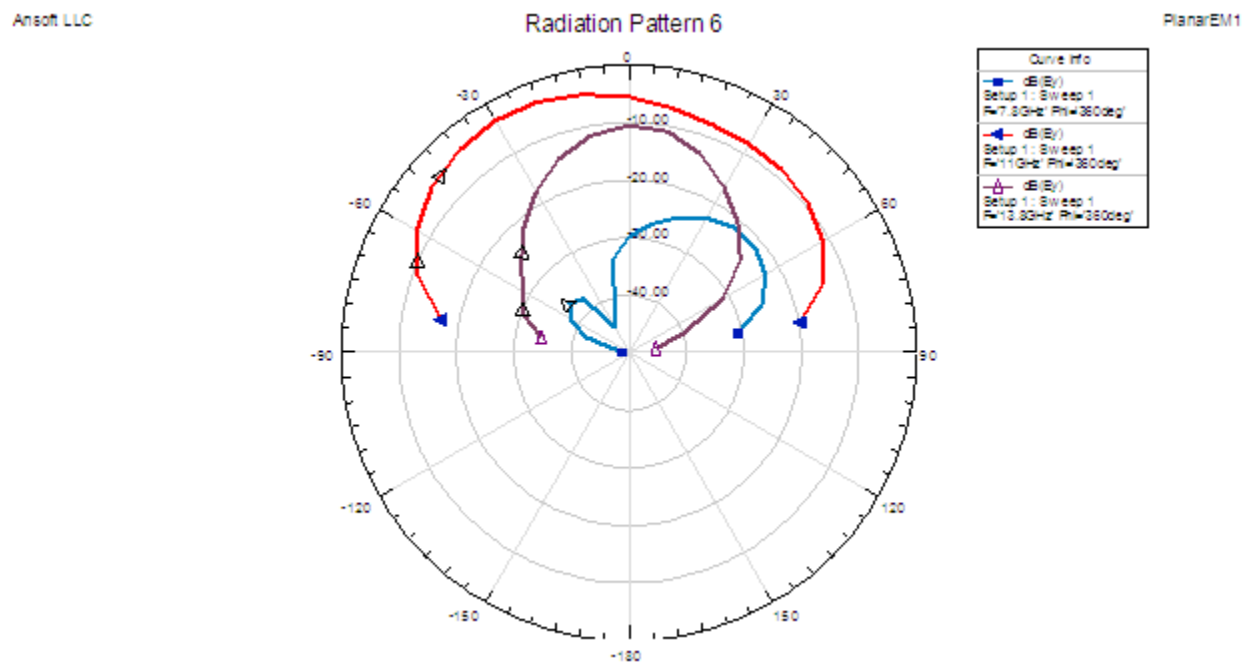


Fig. 6b The simulated surface current distribution and directivity pattern of the antenna with $f = 7.8$ GHz.

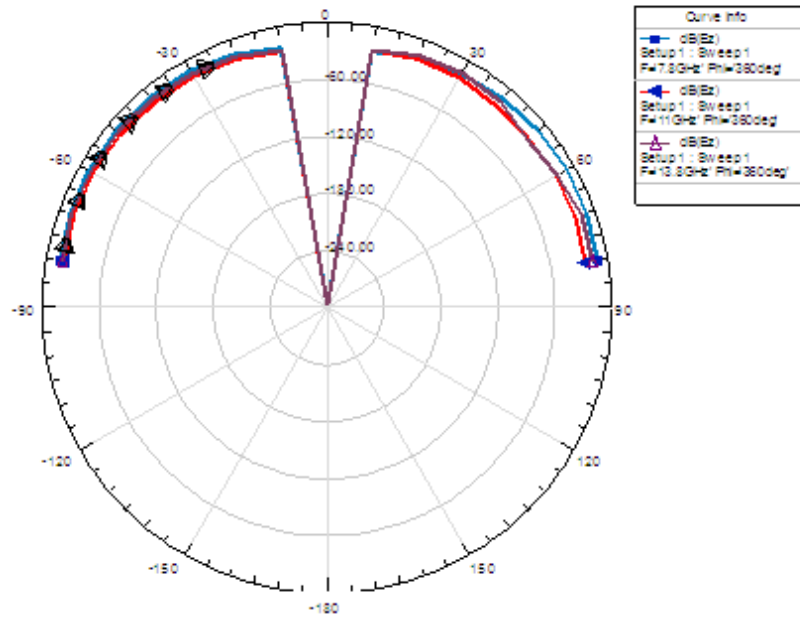
The measured total radiation gain patterns of the fabricated antenna at 13.8, 11 and 7.8 GHz are plotted and compared according to the cutting plane: xy, xz and yz, are shown in the Fig 7.



(a)



(b)



(c)

Fig. 7. Measured total radiation gain patterns: (a) in xy plane, (b) in xz plane, and (c) in yz plane.

The antenna shown in the (Fig. 8) was fabricated with the following parameters: ARLON 25N, $\epsilon_r = 3.38$ and $h = 1.54$ mm and with different gap dimensions from 1 mm, 3 mm to 5 mm.

The measured result was obtained from the laboratory using Agilent Technologies, E8364B, MY43040445 A.04.87.01. The measured return loss antenna is shown in the Fig. 8a.

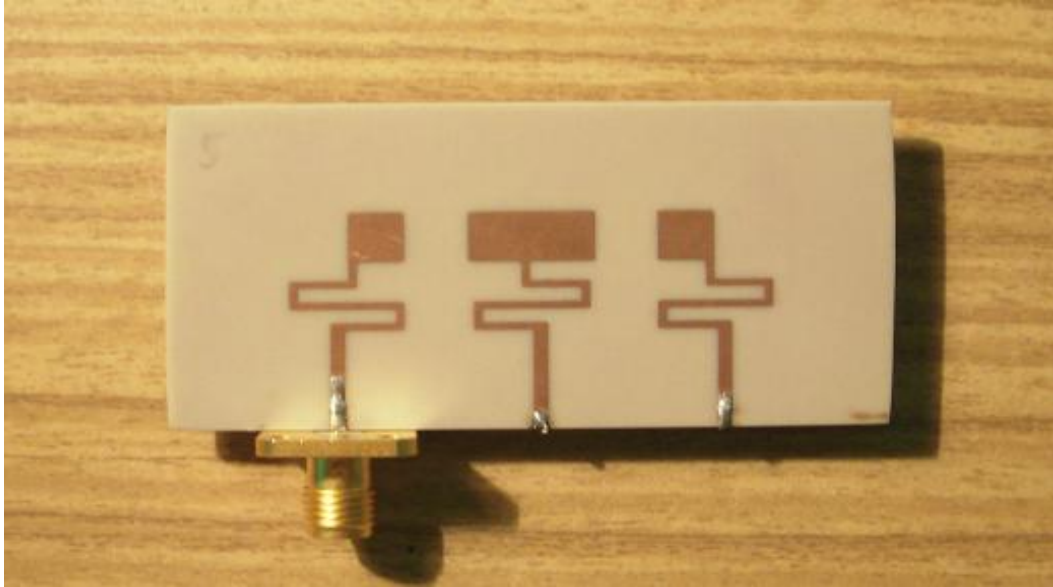


Fig. 8 Photograph of the fabricated prototype antenna

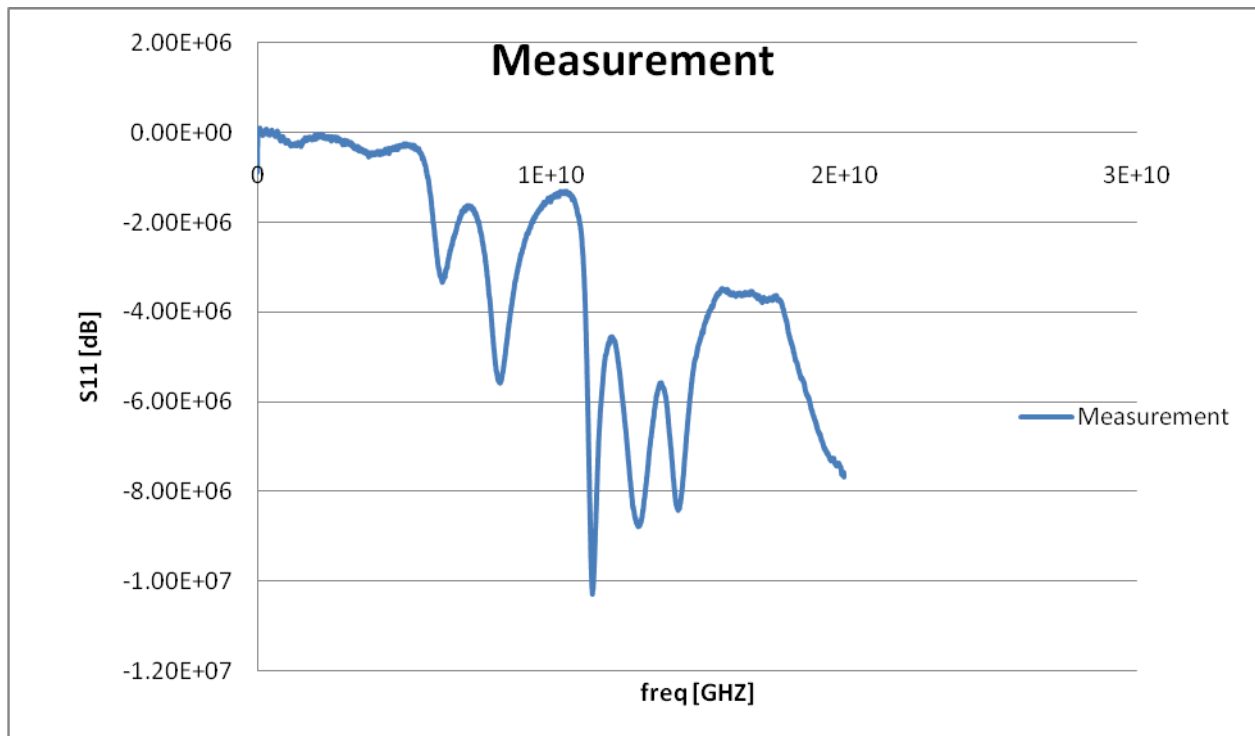


Fig. 8a Measured return loss of antenna.

From the laboratory it was possible to measure the directional characteristics of the fabricated antenna in plane YZ with the frequency 3.4 GHz as shown in the Fig. 9.

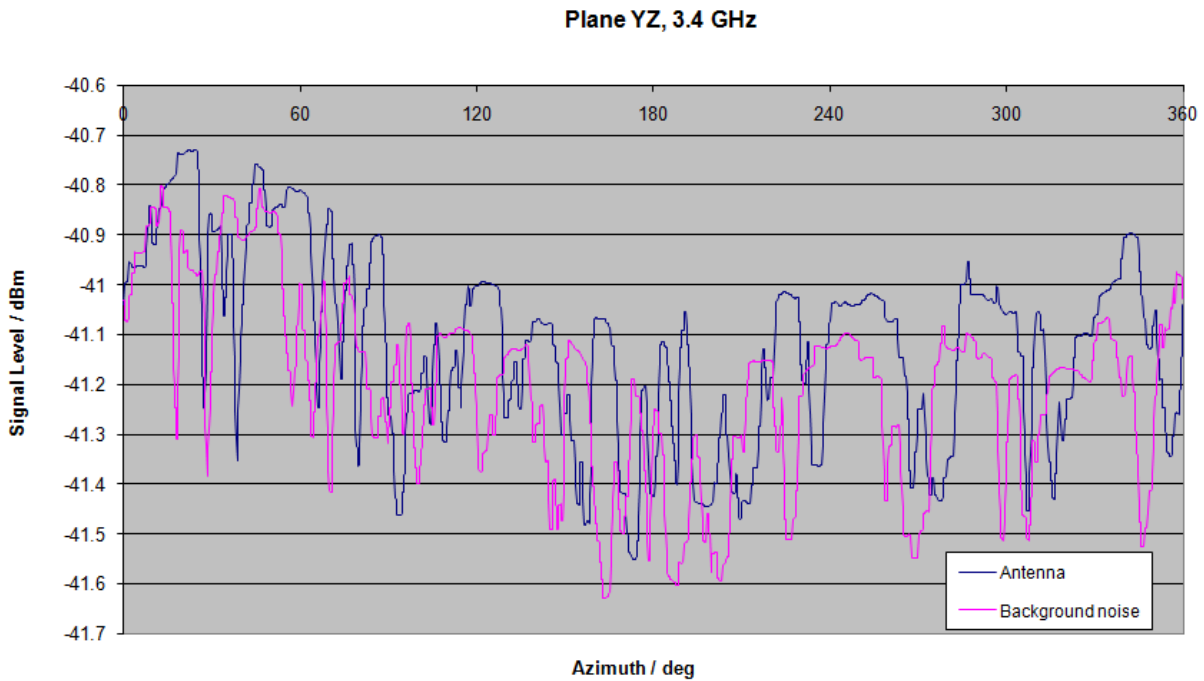


Fig. 9 The measured directional characteristics of antenna with frequency 3.4 GHz.

5 CONCLUSIONS

In this project, I discussed some properties of meta-material antennas, their design and simulation in Ansoft Designer.

Structure of the antenna is depicted in Fig. 2. The resonance was obtained between 7 GHz and 8.9 GHz. Results do not change for the different value of the gap. Corresponding current distributions and directivity patterns are shown in Fig. 6, Fig. 6a and Fig. 6b for different frequencies.

In order to investigate the behavior of the antenna, simulations were performed in frequency range from 2 GHz to 16 GHz with the frequency step 0.2 GHz. This simulations was for all the gap widths $g = 1\text{ mm}$, 3 mm to $g = 5\text{ mm}$.

In the laboratory using Agilent Technologies, E8364B, MY43040445 A.04.87.01 was measured the return loss of antenna for all the gap widths $g = 1\text{ mm}$, 3 mm to $g = 5\text{ mm}$ and the results were the same with the frequencies from 1 GHz to 16 GHz.

REFERENCES

- [1] JI, J. K., KIM, G. H., SEONG, W. M. Bandwidth enhancement of metamaterial antennas based on composite right/left-handed transmission line. *IEEE Antennas and Wireless Propagation Letters*, 2010, vol. 9, no. 5, p. 36–39.
- [2] ENGHETA, N. An idea for thin subwavelength cavity resonators using metamaterials with negative permittivity and permeability. *IEEE Antennas and Wireless Propagation Letters*, 2002, vol. 1, p. 10–13.
- [3] BOSE, J. C. On the rotation of plane polarization of electric waves by a twisted structure. *Proceedings of the Royal Society of London*, 1898, vol. 63, p. 146–152.
- [4] CALOZ, C., ITOH, T. *Electromagnetic Metamaterials: Transmission Line Theory and Microwave Applications*. New York: J. Wiley and Sons, 2006.
- [5] Nader Engheta, Richard W. Ziolkowski *Metamaterials Physics and Engineering Explorations*

LIST OF FIGURES

Fig. 1	Material classifications	7
Fig. 2	Geometry of the scattering of a wave obliquely incident upon a DPS-DNG interface	12
Fig. 3	Equivalent circuit model for the ideal CRLH-TL unit cell	13
Fig. 4	MTM antenna with extended bandwidth	14
Fig. 5	Simulated return loss for the transmission line with the gap width $g = 3$ mm. Analysis performed from 2 GHz to 16 GHz and frequency step 0.2 GHz	15
Fig. 6	The simulated surface current distribution and directivity pattern of the antenna with $f = 13.8$ GHz.	16
Fig. 6a	The simulated surface current distribution and directivity pattern of the antenna with $f = 11$ GHz.	17
Fig. 6b	The simulated surface current distribution and directivity pattern of the antenna with $f = 7.8$ GHz.	17
Fig. 7.	Measured total radiation gain patterns: (a) in xy plane, (b) in xz plane and (c) in yz plane	18
Fig. 8	Photograph of the fabricated prototype antenna	20
Fig. 8a	Measured return loss of antenna.	20
Fig. 9	The measured directional characteristics of antenna with frequency 3.4 GHz.	21

LIST OF SYMBOLS:

MTM	meta-material;
CRL-TL	composite right/left-handed transmission line;
ZOR	zeroth-order resonator;
TL	transmission line;
g	width of the serial gap;
β	the propagation constant of Bloch waves;
d	the length of the unit cell;
N	the number of unit cells of the resonator;
l	the total length of the resonator;
Z_0	characteristic impedance;
C_L	capacitance of the left-handed transmission line;
L_L	inductance of the left-handed transmission line;
C_R	capacitance of the right-handed transmission line;
L_R	inductance of the right-handed transmission line.
A	loop area (square or circular), m^2
C	circumference of circular loop.
L	loop length (perimeter or circumference), m
d	wire or conductor diameter, m
U_θ	radiation intensity in a given direction contained in θ field component
D_ϕ	radiation intensity in a given direction contained in ϕ field component
$(P_{rad})_\theta$	radiated power in all directions contained in θ field component
$(P_{rad})_\phi$	radiated power in all directions contained in ϕ field component.
D	directivity (dimensionless)
D_0	maximum directivity (dimensionless)
U	radiation intensity (W/unit solid angle)
U_{max}	maximum radiation intensity (W/unit solid angle)
U_0	radiation intensity of isotropic source (W/unit solid angle)
P_{rad}	total radiated power (W)
k	efficiency factor ($0 \leq k \leq 1$)
G	gain of an antenna
R_r	radiation resistance
R_L	ohmic losses
ϵ	Permittivity
μ	Permeability
DPS	double-positive medium
ENG	epsilon-negative medium
MNG	mu-negative medium
DNG	double negative medium

IR	infrared
BW	backward-wave media
IEC	International Electrotechnical Commission
IEEE	Institute of Electrical and Electronics Engineers